Theor Chim Acta (1991) 81: 21–30

Theoretica Chimica Acta

Marginal electron density and density-difference functions

Toshikatsu Koga, Kotomi Sano, and Tetsuya Morita

Department of Applied Chemistry, Muroran Institute of Technology, Muroran, Hokkaido 050, Japan

Received October 29, 1990/Accepted December 18, 1990

Summary. For visual analysis of the density reorganization and distortion, the one-dimensional cut $\Delta\varrho(x, y_0, z_0)$ and the two-dimensional cut $\Delta\varrho(x, y, z_0)$ of the three-dimensional electron density difference function $\Delta\varrho(x, y, z)$ are frequently employed. However, these cut functions do not satisfy any sum rules in contrast to the original difference function $\Delta\varrho(x, y, z)$. To avoid this difficulty, the use of the marginal electron density functions $\varrho_x(x)$ and $\varrho_{xy}(x, y)$ and their difference functions $\Delta\varrho_x(x)$ and $\Delta\varrho_{xy}(x, y)$ is proposed. The marginal densities are condensation of the three-dimensional density onto a particular plane or line of our interest, and they satisfy the sum rule (i.e., the conservation of the number of electrons) exactly. Some basic properties of the marginal electron density are clarified for typical diatomic molecular orbitals. An illustrative application is given for the bonding and antibonding processes in the H_2 system.

Key words: Marginal density – Electron density – Density reorganization – Homonuclear diatomics

1. Introduction

The (spinless) electron density function $\varrho(\boldsymbol{r})$ defined by

$$\varrho(\boldsymbol{r}) \equiv N \int |\Psi(\boldsymbol{r}, \sigma_1; \boldsymbol{r}_2, \sigma_2; \ldots; \boldsymbol{r}_N, \sigma_N)|^2 \, d\boldsymbol{r}_2 \ldots d\boldsymbol{r}_N \, d\sigma_1 \ldots d\sigma_N, \tag{1}$$

is frequently used for interpretative purpose in quantum chemistry, where Ψ is a wave function of the N-electron system under consideration. For example, contour maps of the electron density $\varrho(\boldsymbol{r})$ conveniently provide a visual picture of the shapes, sizes, and bonding characteristics in molecules (see e.g., [1]). The density-difference function,

$$\Delta\varrho(\boldsymbol{r}) \equiv \varrho(\boldsymbol{r}) - \varrho_0(\boldsymbol{r}), \tag{2}$$

first introduced by Roux, Besnainou, and Daudel [2], is also employed for a detailed analysis of the density reorganization or distortion upon molecular formation, where $\varrho_0(\boldsymbol{r})$ denotes a reference electron density obtained by the superposition of the constituent atomic densities (see [3] for a review of density

and density-difference functions). Recently, Ruedenberg, Schwarz and coworkers [4] have pointed out the inappropriateness of using spherically-averaged reference atomic densities and developed the method of chemical deformation densities.

Though the number of spatial variables is reduced from $3N$ in the wave function Ψ to three in the density ϱ and the density-difference $\Delta\varrho$, it is still inconvenient for visual analysis to treat ϱ and $\Delta\varrho$ as a function of three independent spatial variables. Therefore, one usually considers a representative plane, e.g., $z = z_0$, and constructs the contour maps of $\varrho(x, y, z_0)$ and $\Delta\varrho(x, y, z_0)$. In some cases, the one-dimensional cuts, e.g., $\varrho(x, y_0, z_0)$ and $\Delta\varrho(x, y_0, z_0)$ are used. In these "reduced" density-difference functions $\Delta\varrho(x, y, z_0)$ and $\Delta\varrho(x, y_0, z_0)$, there usually appear positive and negative parts depending on the region specified by x and y or x alone. One *often interprets* this observation as the result of density migration from one region where $\Delta\varrho$ is negative to the other region where $\Delta\varrho$ is positive. However, it is clear that

$$\int \Delta\varrho(\boldsymbol{r})\, d\boldsymbol{r} = \int \Delta\varrho(x, y, z)\, dx\, dy\, dz = 0, \tag{3a}$$

but

$$\int \Delta\varrho(x, y, z_0)\, dx\, dy \neq 0 \quad \text{and} \quad \int \Delta\varrho(x, y_0, z_0)\, dx \neq 0. \tag{3b}$$

Namely, the sum rule does not hold for the reduced density-difference functions $\Delta\varrho(x, y, z_0)$ and $\Delta\varrho(x, y_0, z_0)$, and hence the correctness of the above interpretation is *not* always guaranteed.

Based on this motivation, we here study the use of marginal electron density and density-difference functions for the analysis of density reorganizations. The marginal functions enable us to reduce the number of variables in the density function to either two or one without violating the sum rule (i.e., the conservation of the number of electrons). The definition of the marginal density and density-difference functions is given in the next section together with their relations to the experimental form factor. In Sect. 3, basic properties of the marginal electron density and density-difference functions are examined for six types of homonuclear diatomic molecular orbitals (MOs) constructed from $1s$ and $2p$ atomic orbitals (AOs). An illustrative application of the marginal density function is presented in Sect. 4 for the analysis of the density reorganizations in the $^1\Sigma_g^+$ and $^3\Sigma_u^+$ states of the H_2 system as a function of the internuclear distance. Atomic units are used throughout this paper.

2. Marginal electron density

The electron density function $\varrho(\boldsymbol{r}) = \varrho(x, y, z)$ defined by Eq. (1) is a joint probability density function with three variables. Then the two-dimensional marginal density function $\varrho_{xy}(x, y)$ with respect to the variables x and y is given by

$$\varrho_{xy}(x, y) \equiv \int \varrho(x, y, z)\, dz, \tag{4}$$

which is a projection of the three-dimensional density $\varrho(x, y, z)$ onto the two-dimensional xy-plane. The other two marginal densities $\varrho_{yz}(y, z)$ and $\varrho_{xz}(x, z)$

are analogously defined. The one-dimensional marginal density is obtained by integrating $\varrho(x, y, z)$ over two variables. For example,

$$\varrho_x(x) \equiv \int \varrho(x, y, z)\, dy\, dz = \int \varrho_{xy}(x, y)\, dy = \int \varrho_{xz}(x, z)\, dz, \tag{5}$$

which is a projection of $\varrho(x, y, z)$ onto a line (the x-axis in this case).

As is well-known, the Fourier transformation of the electron density $\varrho(\boldsymbol{r})$ gives the form factor $F(\boldsymbol{s})$, which determines the coherent or elastic X-ray scattering intensity in the Waller–Hartree theory and the elastic electron-scattering intensity in the first Born approximation [5, 6]:

$$F(\boldsymbol{s}) = \int \exp(i\boldsymbol{s} \cdot \boldsymbol{r})\varrho(\boldsymbol{r})\, d\boldsymbol{r}. \tag{6}$$

If we set $s_z = 0$ in Eq. (6), we have

$$F(s_x, s_y, 0) = \int \exp[i(s_x x + s_y y)]\varrho_{xy}(x, y)\, dx\, dy. \tag{7a}$$

Similarly,

$$F(s_x, 0, 0) = \int \exp(is_x x)\varrho_x(x)\, dx. \tag{7b}$$

Namely, the marginal electron densities have another physical meaning that they are the Fourier transforms of the components of the form factor in the corresponding planes or lines.

Since the marginal densities $\varrho_{xy}(x, y)$ etc. and $\varrho_x(x)$ etc. represent a "condensation" of the three-dimensional density $\varrho(x, y, z)$ onto a particular plane or line of our interest, the number of electrons is conserved; e.g.,

$$\int \varrho(x, y, z)\, dx\, dy\, dz = \int \varrho_{xy}(x, y)\, dx\, dy = \int \varrho_x(x)\, dx = N. \tag{8}$$

As a result, the marginal density-difference functions do satisfy the sum rule

$$\int \Delta\varrho_{xy}(x, y)\, dx\, dy = \int \Delta\varrho_x(x)\, dx = 0, \text{ etc.}, \tag{9}$$

where

$$\Delta\varrho_{xy}(x, y) \equiv \int \Delta\varrho(x, y, z)\, dz, \tag{10a}$$

$$\Delta\varrho_x(x) \equiv \int \Delta\varrho(x, y, z)\, dy\, dz, \tag{10b}$$

and so on. When we employ the difference in marginal electron densities, Eq. (9) therefore allows the interpretation that the density flow has occurred from one region to the other based on the negativity and positivity observed in the difference function.

3. Marginal electron density for homonuclear diatomic MOs

In order to study the fundamental properties of the marginal electron density and density-difference functions, we examine six typical MOs appearing in

homonuclear diatomics:

$$\psi_{\pm}(\boldsymbol{r}) = (2 \pm 2S)^{-1/2}[\chi_a(\boldsymbol{r}) \pm \chi_b(\boldsymbol{r})], \quad S = \langle \chi_a | \chi_b \rangle, \tag{11}$$

where χ_a and χ_b are similar AOs centered on a and b separated by the vector $\boldsymbol{R}$, i.e., $\chi_a(\boldsymbol{r}) \equiv \chi(\boldsymbol{r} + \boldsymbol{R}/2)$ and $\chi_b(\boldsymbol{r}) \equiv \chi(\boldsymbol{r} - \boldsymbol{R}/2)$. The Slater-type functions are assumed for the AOs χ:

$$\chi_{nlm}(\boldsymbol{r}) = (2n)!(2\zeta)^{n+1/2} r^{n-1} \exp(-\zeta r) Y_{lm}(\theta, \phi), \tag{12}$$

where (r, θ, ϕ) is the spherical polar coordinates of $\boldsymbol{r}$ and Y_{lm} is the spherical harmonic [7].

For the $\sigma_g 1s$ MO, the two-dimensional marginal density $\varrho_{xz}(x, z)$ is compared in Fig. 1 with the two-dimensional cut $\varrho(x, 0, z)$. The difference functions $\Delta\varrho_{xz}(x, z)$ and $\Delta\varrho(x, 0, z)$ are also given there, where the reference density $\varrho_0(\boldsymbol{r})$ has been defined by

$$\varrho_0(\boldsymbol{r}) = (1/2)[|\chi_a(\boldsymbol{r})|^2 + |\chi_b(\boldsymbol{r})|^2]. \tag{13}$$

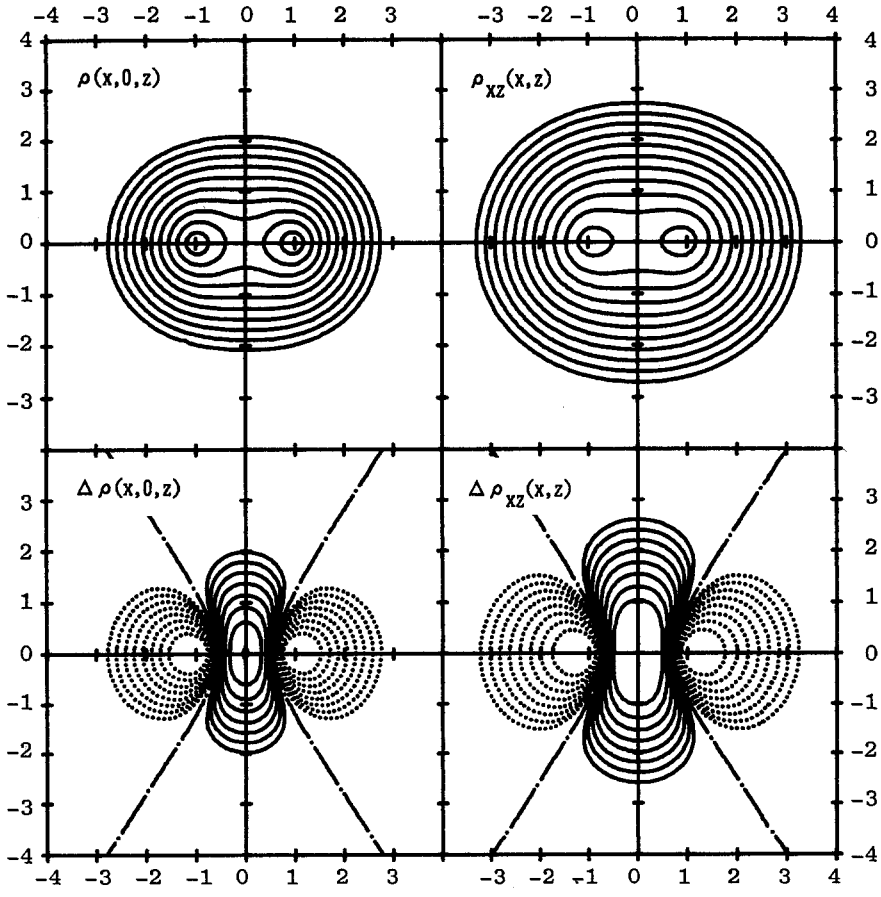

Fig. 1. Comparison of $\varrho(x, 0, z)$ with $\varrho_{xz}(x, z)$, and $\Delta\varrho(x, 0, z)$ with $\Delta\varrho_{xz}(x, z)$ for the $\sigma_g 1s$ MO. Contour values are $2^{-n/2}$ ($n = 6, 7, \ldots, 17$) for the densities, and 0 and $\pm 2^{-n/2}$ ($n = 13, 14, \ldots, 20$) for the density differences. *Dotted lines* represent negative values

The integration over the y coordinate involved in $\varrho_{xz}(x, z)$ and $\Delta\varrho_{xz}(x, z)$ has been performed based on the 10-term Gaussian expansion [8] of the Slater-type function. (For simplicity, we set $\boldsymbol{R} = (0, 0, 2)$ and $\zeta = 1$ throughout this section.) For the distributions given in Fig. 1, we obtain after numerical integrations

$$\int \varrho_{xz}(x, z)\, dx\, dz = 1.000, \qquad \int \Delta\varrho_{xz}(x, z)\, dx\, dz = 0.000, \tag{14a}$$

but

$$\int \varrho(x, 0, z)\, dx\, dz = 0.475, \qquad \int \Delta\varrho(x, 0, z)\, dx\, dz = -0.025. \tag{14b}$$

Indeed, we see the cut functions $\varrho(x, 0, z)$ and $\Delta\varrho(x, 0, z)$ are far from sum rules; $\Delta\varrho(x, 0, z)$ emphasizes the density decrease behind the nuclei too much. However, the qualitative features in $\varrho(x, 0, z)$ and $\varrho_{xz}(x, z)$ and in $\Delta\varrho(x, 0, z)$ and $\Delta\varrho_{xz}(x, z)$ are very similar. Both the $\varrho(x, 0, z)$ and $\varrho_{xz}(x, z)$ reveal ellipsoidal distributions corresponding to the σ-bonding situation. Accordingly, the difference functions show the density migration from the regions behind the nuclei to the region between the nuclei. Consequently, the two-dimensional marginal density does not seem to give a new insight for the electron density (re)distribution at least for the $\sigma_g 1s$ MO.

On the other hand, the one-dimensional marginal density $\varrho_z(z)$ is quite different from $\varrho(0, 0, z)$. Figure 2 compares $\varrho_z(z)$ and $\varrho(0, 0, z)$ for the six MOs constructed from the $1s$ and $2p$ AOs. The integrations over the x and y coordinates involved in $\varrho_z(z)$ can be directly performed for the Slater-type function (12) and we obtain a closed-form expression for $\varrho_z(z)$. For example, we have

$$\begin{aligned}\varrho_z(z) = [\zeta/(4 + 4S)]\{&\Gamma(2, 2\zeta|z + R/2|) + \Gamma(2, 2\zeta|z - R/2|) \\ &+ 2\Gamma(2, \zeta|z + R/2| + \zeta|z - R/2|) \\ &- 8\zeta^4 z^2 R^2 \Gamma(-2, \zeta|z + R/2| + \zeta|z - R/2|)\},\end{aligned} \tag{15}$$

for the $\sigma_g 1s$ MO, where $R = |\boldsymbol{R}|$ and $\Gamma(n, x)$ is the incomplete gamma function [9],

$$\Gamma(n + 1, x) = n! \exp(-x) \sum_{i=0}^{n} (x^i/i!) \quad (n \geqslant 0), \tag{16a}$$

$$\Gamma(-n, x) = [(-1)^n/n!]\left\{\Gamma(0, x) - \exp(-x) \sum_{i=0}^{n-1} [(-1)^i i!/x^{i+1}]\right\} \quad (n > 0). \tag{16b}$$

For the $\sigma_g 1s$ MO, we first note that the cusps in $\varrho(0, 0, z)$ do not appear in $\varrho_z(z)$. We also find that the marginal density $\varrho_z(z)$ shows a larger density accumulation in the internuclear region than $\varrho(0, 0, z)$. Actually, $\varrho_z(z)$ has a nearly-flat distribution between the nuclei, and this implies that the density distribution off the internuclear axis gives a nontrivial contribution to the bonding. Similarly, for the antibonding $\sigma_u 1s$ MO, $\varrho_z(z)$ has no cusp and shows a greater amount of the density behind the nuclei. The emphasis of the bonding and antibonding electron density contributions in $\varrho_z(z)$ is also observed for the $\sigma_g 2p$ and $\sigma_u 2p$ MOs. The marginal densities $\varrho_z(z)$ for the $\pi_u 2p$ and $\pi_g 2p$ MOs are found to be relatively similar to those of the $\sigma_g 1s$ and $\sigma_u 1s$ MOs, respectively. This fact again shows the importance of the contribution of the density off the internuclear axis which

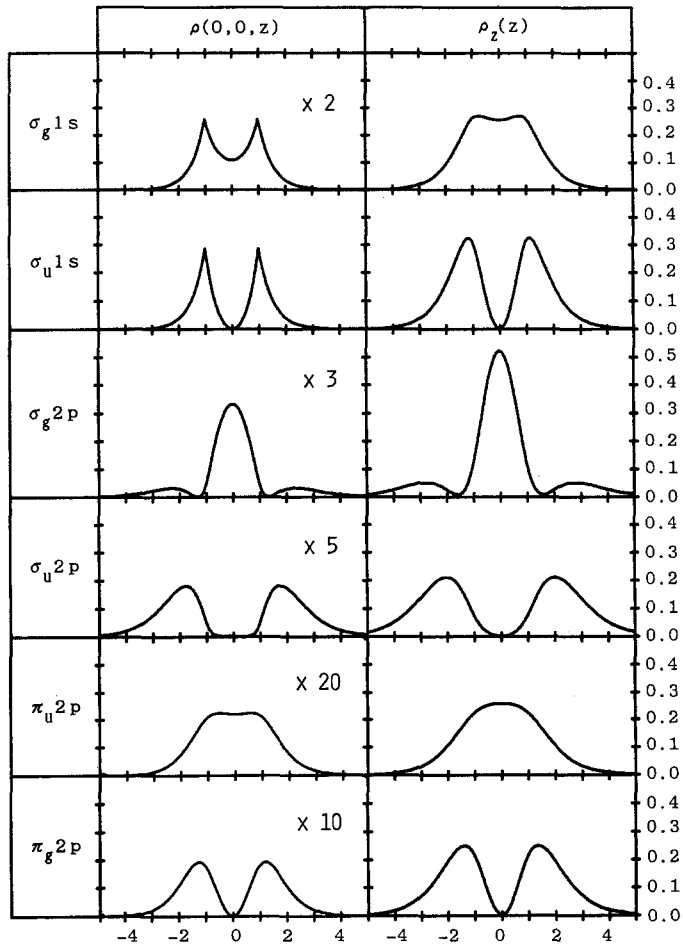

Fig. 2. Comparison of $\varrho(0, 0, z)$ and $\varrho_z(z)$ for the six homonuclear diatomic MOs constructed from the $1s$ and $2p$ AOs. For the π MOs, $\varrho(1, 0, z)$ is presented

does not appear in $\varrho(0, 0, z)$. In this relation, it is significant that in contrast to the function $\varrho(0, 0, z)$, the marginal density $\varrho_z(z)$ enables us to discuss the σ and π (and other) densities on an equal footing. We note that $\int \varrho_z(z)\, dz = 1$ for all MOs given in Fig. 2, but $\int \varrho(0, 0, z)\, dz$ is 0.282, 0.457, 0.196, and 0.136 for the $\sigma_g 1s$, $\sigma_u 1s$, $\sigma_g 2p$, and $\sigma_u 2p$ MOs, respectively.

The density-difference functions $\Delta\varrho(0, 0, z)$ and $\Delta\varrho_z(z)$ are compared in Fig. 3. In accord with the features found in Fig. 2, $\Delta\varrho_z(z)$ has a tendency to emphasize the density reorganization accompanied by the bonding or antibonding nature of the individual MOs; this is much clearer in $\Delta\varrho_z(z)$ than in $\Delta\varrho(0, 0, z)$. In particular, $\Delta\varrho_z(z)$ shows that the density migrations in the $\sigma_g 2p$ and $\sigma_u 2p$ MOs are considerably larger than those expected from $\Delta\varrho(0, 0, z)$. It may be also interesting to see that the reorganizations in the $\pi 2p$ MOs are comparable to those in the $\sigma 1s$ MOs. The integrations give $\int \Delta\varrho_z(z)\, dz = 0$ for all MOs, but $\int \Delta\varrho(0, 0, z)\, dz = -0.036$, 0.139, 0.037, and -0.023, respectively, for the $\sigma_g 1s$, $\sigma_u 1s$, $\sigma_g 2p$, and $\sigma_u 2p$ MOs, and the failure of the sum rule is evident for the cut function $\Delta\varrho(0, 0, z)$.

These studies show that the one-dimensional marginal density $\varrho_z(z)$ and its difference function $\Delta\varrho_z(z)$ provide us with a new view of the density distribution

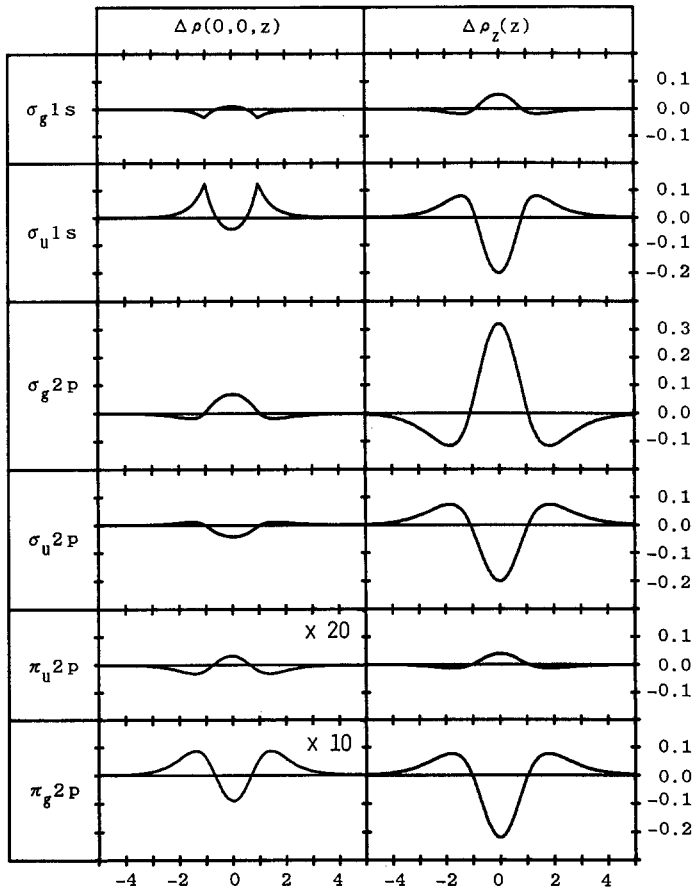

Fig. 3. Comparison of $\Delta\varrho(0, 0, z)$ and $\Delta\varrho_z(z)$ for the six homonuclear diatomic MOs constructed from the $1s$ and $2p$ AOs. For the π MOs, $\Delta\varrho(1, 0, z)$ is presented

and reorganization that differs from the picture hitherto considered based on $\Delta\varrho(0, 0, z)$. Since our above analysis has been restricted to $R = 2$ and $\zeta = 1$, an examination of a realistic system based on $\varrho_z(z)$ and $\Delta\varrho_z(z)$ is desired. Such a study is presented in the next section for the prototypical bonding and antibonding processes in the H_2 system.

4. Marginal electron density in H_2 system

We apply the marginal density analysis to the bonding ($^1\Sigma_g^+$) and antibonding ($^3\Sigma_u^+$) states of the H_2 system as a function of the internuclear distance R. The Weinbaum function [10] is used as the parent wave function, which consists of the covalent and ionic terms. For the bonding singlet state, the spatial function is given by

$$^1\Psi(r_1, r_2) = (1 + C^2 + 2C\langle\Phi_C|\Phi_I\rangle)^{-1/2}[\Phi_C(r_1, r_2) + C\Phi_I(r_1, r_2)], \tag{17a}$$

$$\Phi_C(r_1, r_2) = (2 + 2S^2)^{-1/2}[\chi_a(r_1)\chi_b(r_2) + \chi_b(r_1)\chi_a(r_2)], \tag{17b}$$

$$\Phi_I(r_1, r_2) = (2 + 2S^2)^{-1/2}[\chi_a(r_1)\chi_a(r_2) + \chi_b(r_1)\chi_b(r_2)], \tag{17c}$$

where $S = \langle \chi_a | \chi_b \rangle$ and where χ_a and χ_b are $1s$ Slater functions with the exponent ζ (i.e., χ_{100} in Eq. (12)) centered on the nuclei a and b. For a given R, the two parameters ζ and C are variationally determined. (The Weinbaum function (17) yields the equilibrium distance $R_e = 1.430$ with the total energy $E = -1.147937$ for $\zeta = 1.19378$ and $C = 0.26448$.) For the antibonding triplet state, the ionic term does not contribute by the symmetry requirement and the spatial function is given by

$$^3\Psi(r_1, r_2) = (2 - 2S^2)^{-1/2}[\chi_a(r_1)\chi_b(r_2) - \chi_b(r_1)\chi_a(r_2)], \tag{18}$$

which is identical with the Wang function [11]. Corresponding to Eqs. (17) and (18), the three-dimensional electron density functions $^1\varrho(r)$ and $^3\varrho(r)$ are obtained:

$$^1\varrho(r) = \{(1 + C^2 + 2CS)[\chi_a(r)^2 + \chi_b(r)^2] + 2[2C + S(1 + C^2)]\chi_a(r)\chi_b(r)\} \\ /[(1 + S^2)(1 + C^2) + 4CS], \tag{19a}$$

$$^3\varrho(r) = [\chi_a(r)^2 + \chi_b(r)^2 - 2S\chi_a(r)\chi_b(r)]/(1 - S^2). \tag{19b}$$

The reference density $\varrho_0(r)$ is a superposition of the two $1s$ densities located at a and b with the exponent $\zeta = 1$, corresponding to the two ground-state hydrogen atoms:

$$\rho_0(r) = \chi_a(r; \zeta = 1)^2 + \chi_b(r; \zeta = 1)^2. \tag{20}$$

Figure 4 compares the one-dimensional density-difference functions $\Delta\varrho(0, 0, z)$ and $\Delta\varrho_z(z)$ for the selected internuclear distances in the bonding state.

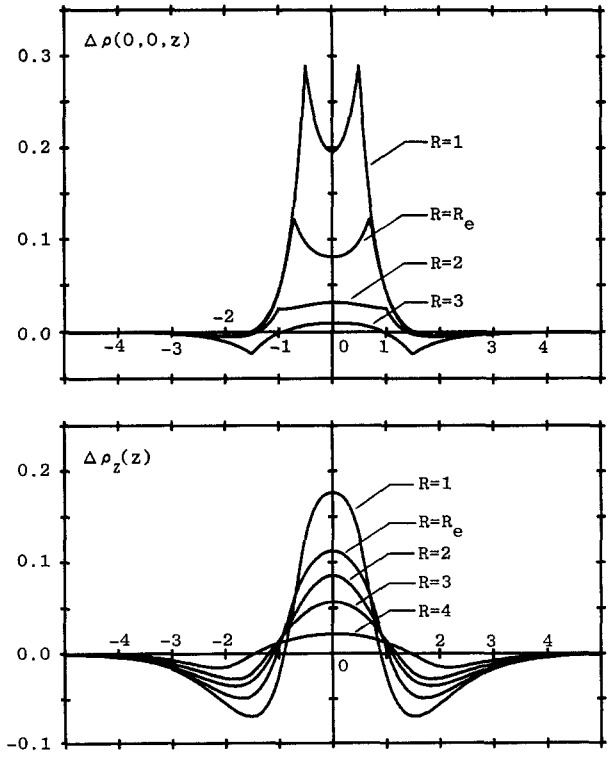

Fig. 4. Density reorganization in terms of the marginal density $\Delta\varrho_z(z)$ for the bonding $^1\Sigma_g^+$ state of the H_2 system

The cut function $\Delta\varrho(0, 0, z)$ reveals an expected bonding characteristic that the electron density increases gradually in the internuclear region as the distance R diminishes. However, $\Delta\varrho(0, 0, z)$ emphasizes the density increase, and the density decrease in the regions behind the nuclei is very small. Actually, we have $\int \Delta\varrho(0, 0, z)\, dz = 0.051$, 0.182, and 0.361 for $R = 2$, R_e, and 1, respectively. Moreover, the $\Delta\varrho(0, 0, z)$ function suggests that the largest density accumulation occurs at the nuclear positions for $R = R_e$ and 1. These trends have also been observed [12, 13] in the analysis based on a more accurate wave function. On the other hand, the marginal function $\Delta\varrho_z(z)$ clearly shows the density migration accompanied by the bonding interaction; the electron density flows from the region behind to the region between the nuclei. The amounts of the density increase and decrease are exactly equal by the definition of the marginal density (Eq. (9)). The most striking feature of $\Delta\varrho_z(z)$ is that the largest density accumulation occurs at the center of the two nuclei. The peak height increases as the interaction increases (i.e., R decreases). Since the marginal density also takes into account the density change off the internuclear axis, the density reorganizations described by $\Delta\varrho_z(z)$ appear to be a more realistic description of the bonding density reorganization than those of $\Delta\varrho(0, 0, z)$.

The corresponding density analysis for the antibonding $^3\Sigma_u^+$ state is presented in Fig. 5. The cut function $\Delta\varrho(0, 0, z)$ shows the density flow from the internuclear region to the outside-the-nuclei regions, reflecting the antibonding nature. However, $\int \Delta\varrho(0, 0, z)\, dz$ is calculated to be 0.040, 0.077, and 0.069 for $R = 3$, 2 and 1, and the $\Delta\varrho(0, 0, z)$ function underestimates the density decrease in the

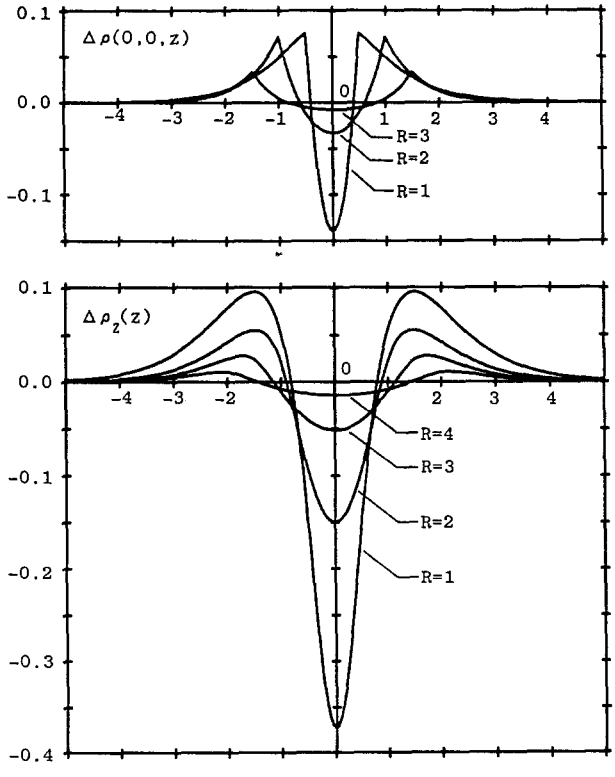

Fig. 5. Density reorganization in terms of the marginal density $\Delta\varrho_z(z)$ for the antibonding $^3\Sigma_u^+$ state of the H_2 system

internuclear region. The marginal density-difference function $\Delta\varrho_z(z)$ improves this defect and shows the outward density migration in a consistent manner. $\Delta\varrho_z(z)$ shows that the density decrease in the internuclear region is much larger than that expected from $\Delta\varrho(0, 0, z)$. The overall change in $\Delta\varrho_z(z)$ is approximately opposite to that observed for the bonding state (Fig. 4), but the density decrease around the center of the nuclei is sharper than the corresponding increase in the bonding state.

In summary, we have studied the use of the marginal density functions $\varrho_{xz}(x, z)$ and $\varrho_z(z)$ and their difference functions for the analysis of the electron density distribution and reorganization. The examination of the six homonuclear diatomic MOs has shown that the functions $\varrho_z(z)$ and $\Delta\varrho_z(z)$ provide more realistic density information than the usual cut functions $\varrho(0, 0, z)$ and $\Delta\varrho(0, 0, z)$. Applications to the typical bonding and antibonding interaction processes in the H_2 system have illustrated that the $\Delta\varrho(0, 0, z)$ function usually employed gives an incorrect impression of the amount and location of the density migration. We may conclude that the marginal density, which satisfies the definite sum rule, is useful for the quantitative analysis of the electron density redistribution.

References

1. Bader RFW, Henneker WH, Cade PE (1967) J Chem Phys 46:3341
2. Roux M, Besnainou S, Daudel R (1956) J Chim Phys 53:218
3. Bader RFW (1975) In: Buckingham AD, Coulson CA (eds) International review of science: Theoretical chemistry: Physical Chemistry, ser. 2, vol. 1. Butterworths, London, pp 43–78
4. Schwarz WHE, Valtazanos P, Ruedenberg K (1985) Theor Chim Acta 68:471; Schwarz WHE, Ruedenberg K, Mensching L (1989) J Am Chem Soc 111:6926; Mensching L, Von Niessen W, Valtazanos P, Ruedenberg K, Schwarz WHE (1989) J Am Chem Soc 111:6933; Schwarz WHE, Ruedenberg K, Mensching L, Miller LL, Valtazanos P, Von Niessen W, Jacobson R (1989) Angew Chen Int Ed Eng 28:597; Ruedenberg K, Schwarz WHE (1990) J Chem Phys 92:4956
5. Benesch R, Smith Jr VH (1970) Acta Crystallogr Sect A 26:579
6. Benesch R, Smith Jr VH (1973) In: Price WC, Chissick SS, Ravensdale T (eds) Wave mechanics: The first fifty years. Butterworths, London, pp 357–377
7. Messiah A (1961) Quantum mechanics, vol. 1. North-Holland, Amsterdam, pp 494–496
8. O-ohata K, Taketa H, Huzinaga S (1966) J Phys Soc Jpn 21:2306
9. Gradshteyn IS, Ryzhik IM (1980) Table of integrals, series, and products. Academic, New York, pp 940–942
10. Weinbaum S (1933) J Chem Phys 1:593
11. Wang SC (1928) Phys Rev 31:579
12. Bader RFW, Chandra AK (1968) Can J Chem 46:953
13. Bader RFW (1970) An introduction to the electronic structure of atoms and molecules. Clarke, Irwin & Co, Toronto, p 134